Dalton Transactions

PAPER

View Article Online
View Journal

Cite this: DOI: 10.1039/c5dt02049b

Computational and carbon-13 NMR studies of Pt–C bonds in P–C–P pincer complexes†

Yu-Xiang Jia, Xiang-Yuan Yang, Wee Shan Tay, Yongxin Li, Sumod A. Pullarkat, Kai Xu, Hajime Hirao and Pak-Hing Leung*

Received 30th May 2015,
Accepted 7th October 2015

DOI: 10.1039/c5dt02049b

www.rsc.org/dalton

A $^{13}C\{^1H\}$ NMR based investigation was conducted to examine the electronic properties of C(aryl)–M bonds and their *trans* influence in P–C(aryl)–P pincer complexes. A series of structurally related platinum pincer complexes were rationally designed and their corresponding $^{13}C-^{195}Pt$ coupling constants were systematically examined. By methodical substitution of the ligand *trans* to the organometallic C(aryl)–Pt bond, this study revealed the significant influence of the ligands on the nature of the C(aryl)–M bonds. The single crystal X-ray analysis of the complexes and computational studies further confirmed the observations that the C–M bond exhibits significant π-character.

Introduction

The important role played by phosphorus ligands in transition metal catalyzed organic synthesis is well established. Many well-established diphosphine ligands, such as BINAP, DIPAMP and CHIRAPHOS are able to efficiently project their well-defined structural features to control the stereochemistry during the course of the asymmetric reaction.[1] It needs to be noted that the soft phosphorus atoms of these diphosphines readily function as both σ-donors as well as π-acceptors. This particular donor–acceptor property renders phosphine ligands as ideal catalyst-supporters. This dual role is especially critical for reactions in which the mechanisms involve vast changes in electronic density, such as oxidative addition of substrates and reductive elimination of products. Noticeably, the active catalytic sites of diphosphine–metal catalysts are typically located *trans* to the phosphorus donors.

Similar to their diphosphine analogues, square–planar metal complexes (Fig. 1, type 1) supported by P–C–P ligands frequently demonstrate high stability and attractive catalytic properties.[2] The pincer catalysts can direct their stereocontrol efficiently *via* their pincer arms or from the chirality of the phosphorus donors. Therefore, for a catalytic process that does not involve changes in the coordination geometry of the P–C–P pincer catalyst, the stereochemistry of the sole M–X catalytic site can be rationally controlled by a specially designed pincer ligand. In contrast to the aforementioned diphosphine ligands, the active catalytic site in the P–C–P complex (type 1) is the coordination position *trans* to the aromatic carbon. The two phosphorus donors in the P–C–P complex occupy the positions *cis* relative to the catalytic site. Due to the symmetry of the d-orbitals, it is well established that square–planar and octahedral transition metal complexes exert much stronger *trans* electronic influences than the analogous *cis* interactions. Therefore the (C)aryl–M bonds in type 1 complexes are the most important and direct contributors to the activation of substrates in catalytic processes.

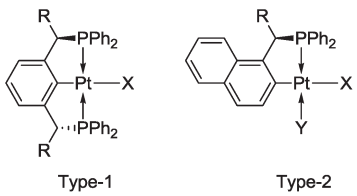

Fig. 1 PCP- and PC-type Pt complexes.

Despite the substantial development of P–C(aryl)–P pincer complexes since the late 1970s, relatively little attention has been directed towards the electronic properties of the M–C bonds or their *trans* influences in catalysis. Roddick and co-workers used $\nu(C{\equiv}O)$ vibrational spectroscopy to study the electronic properties of *trans*-C–M–C≡O pincer complexes bearing different phosphorus substituents in the *cis* positions.[3] Several groups also studied the electrochemistry of similar complexes.[3a] A review of the literature revealed that, based on the solid state structural features, monodentate (C)aryl–M bonds are often described as simple C → M σ-bonds.[4]

Division of Chemistry & Biological Chemistry, School of Physical and Mathematical Sciences, Nanyang Technological University, Singapore 637371.
E-mail: pakhing@ntu.edu.sg

† Electronic supplementary information (ESI) available: Experimental and spectral data, crystallographic refinement data and computational data. CCDC 1401358 (**6a**) and 1401359 (**6c**). For ESI and crystallographic data in CIF or other electronic format see DOI: 10.1039/c5dt02049b

The aryl ligands in these reported C(aryl)–M complexes are inherently free to rotate around the organometallic bond. In contrast, the central aryl-rings in (type 1) pincer complexes are structurally rigid, particularly when the pincer side arms contain substituents which restrict the 5-membered P–C ring conformations. Consequently, the central aromatic ring and the square–planar pincer complexes are expected to be locked into co-planar geometries. We believe that this structurally rigid framework makes it possible for the appropriate π or π* orbitals of the aromatic ring to overlap effectively with the metal d-orbitals, thus directly influencing the electronic properties at the M–X catalytic site. Indeed, we have recently established such π-bonding characters in a group of related *ortho*-metalated (Fig. 1, type 2) complexes.[5] In these complexes, the π* orbitals of the highly conjugated aromatic rings overlap with the metal orbitals, thus rendering a strong *trans*-electronic withdrawing effect directed towards the organometallic M–C bonds. Accordingly, the *trans* C–M–X coordination position shows a preferential affinity towards π-donating moieties, such as oxygen atoms in sulfoxides, ketones, amides and even those in the classic non-coordinating perchlorate anion.[6] Notably, the cyclometalated (type 2) complexes also exhibit typical Lewis acid properties and can be utilized effectively for the catalytic activation of dienophiles and Michael acceptors.[7] We therefore decided to conduct a detailed study in order to determine whether similar π-C–M bonding characters indeed occur in the less conjugated (type 1) pincer complexes. Insights gained from such a detailed investigation is central to understanding the electronic properties of these organometallic bonds and consequently to the future design of pincer complexes as chiral catalysts for asymmetric transformations.

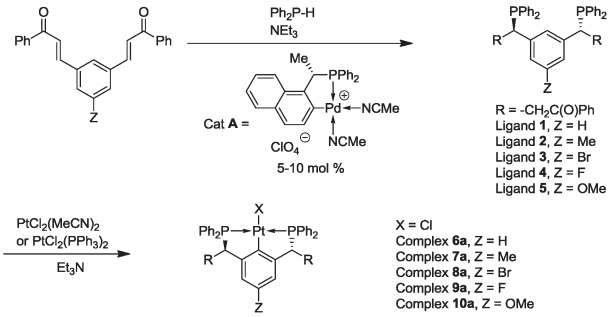

Scheme 1 Syntheses of the pincer ligands and their Pt complexes.

Table 1 Selected NMR data for the pincer-Pt complexes[a]

Complexes [6/7/8]	$^{13}C\{^1H\}$ and $^{31}P\{^1H\}$ NMR data	**6** (Z = H)	**7** (Z = Me)	**8** (Z = Br)
[**a**], X = Cl	δ ^{13}C–^{195}Pt (ppm)	145.9	142.0	145.1
	$^1J_{Pt–C}$ (Hz)	936	944	955
	$^1J_{Pt–PPh_2}$ (Hz)	2967	2974	2935
[**b**] (ClO_4),	δ ^{13}C–^{195}Pt (ppm)	157.8	154.6	157.0
X = PPh_3	$^1J_{Pt–C}$ (Hz)	688	688	703
	trans-($^2J_{C_{ipso}–P}$) (Hz)	90	90	91
	$^1J_{Pt–PPh_3}$ (Hz)	2055	2057	2085
	$^1J_{Pt–PPh_2}$ (Hz)	2768	2775	2743
[**c**], X = CN	δ ^{13}C–^{195}Pt (ppm)	159.5	155.9	158.7
	$^1J_{Pt–C}$ (Hz)	677	677	688
	$^1J_{Pt–PPh_2}$ (Hz)	2781	2790	2757
[**d**], X = NO_3	δ ^{13}C–^{195}Pt (ppm)	135.3	131.3	134.8
	$^1J_{Pt–C}$ (Hz)	951	947	966
	$^1J_{Pt–PPh_2}$ (Hz)	3086	3099	3057

[a] All NMR spectra were recorded in $CDCl_3$ except for complexes **6d–8d**, which were recorded in acetone-d_6.

Results and discussion

In view of the fact that most of the catalytic asymmetric syntheses are conducted in homogeneous solutions, it is our judgment that the determination of the C–M bond properties in solution is of paramount importance. For this specific purpose, $^{13}C\{^1H\}$ NMR spectroscopy is an ideal and powerful tool for the direct investigation of the organometallic bonds in diamagnetic pincer complexes. It should be noted that although the natural abundance of ^{13}C is only about 1.1%, the simple nuclear spin of this isotope generates readily interpretable signals. Furthermore, the carbon atom involved in the C–M bond in these pincer complexes is located at the central position of the two conjoined 5-membered chelates. As routinely observed from the analogous $^{31}P\{^1H\}$ NMR spectroscopy, this unique structural feature allows the C–M ($^{13}C\{^1H\}$) resonance signals to exhibit characteristic high "coordination shifts" and thus renders them generally discernible from the other aromatic carbon signals within the pincer framework.[8] In order to focus on the nature of the C–M bonds, we designed and prepared a series of platinum(II) pincer complexes for $^{13}C\{^1H\}$ NMR investigations (Scheme 1 and Table 1). The ^{13}C–^{195}Pt coupling constants determined from NMR measurements serve as the most direct and reliable indicators for the bond strengths of these organometallic bonds in solution.

The designed pincer ligands can be obtained in high yields with excellent optical purities from the hydrophosphination reaction of the corresponding diketones by using a P–C cyclometalated catalyst (Scheme 1). The pincer ligands are powerful sequesters for platinum(II) ions. The reactions between $PtCl_2(MeCN)_2$ or $PtCl_2(PPh_3)_2$ and the generated ligands in the presence of triethylamine generated highly stable chloro complexes **6a–10a** in high yields.[2c,7b] For a systematic investigation of the *trans* electronic influence on the organometallic C–Pt bond, the chloro ligands in complexes **6a–8a** were subsequently replaced by the anionic CN, NO_3 and the neutral PPh_3 ligands.

As anticipated, the ^{13}C–^{195}Pt signals of the synthesized series of platinum pincer complexes are clearly identified in the $^{13}C\{^1H\}$ NMR spectra. Interestingly, in the 100 MHz $^{13}C\{^1H\}$ NMR spectra, the pincer carbon donors of almost all these platinum complexes do not show any spin–spin coupling with the two identical adjacent P atoms in the square–planar complexes. Complex **8c** is the only complex that shows a very

small coupling constant ($^2J_{P-C}$ = 2 Hz) between the *cis* orientated donors.

Typically, the pincer carbon signals appear as a singlet associated with a pair of platinum satellites at distinctly high chemical shifts. For example, the $^{13}C\{^1H\}$ NMR spectrum of complex **6a** exhibits the C–Pt signal as a singlet signal at δ 145.9 which is, importantly, accompanied by a pair of clearly visible platinum satellites ($^1J_{Pt-C}$ = 936 Hz) (Fig. 2a). However, the pincer aryl carbon shows the expected coupling to the sole *trans* phosphorus donor in complex **6b**. The cationic complex **6b** was prepared by replacing the chloro ligand in complex **6a** with a PPh_3 ligand. The $^{13}C\{^1H\}$ NMR spectrum of complex **6b** clearly shows C_{ipso}–P coupling (90 Hz) between the two *trans* donor atoms (Fig. 2c). Interestingly, the $^1J_{Pt-C}$ coupling observed from PPh_3 complex **6b** ($^1J_{Pt-C}$ = 688 Hz) is markedly weaker than that recorded for complex **6a** (936 Hz). The $^{13}C\{^1H\}$ NMR study shows that the $^1J_{Pt-C}$ coupling constant is further reduced in complex **6c** ($^1J_{Pt-C}$ = 677 Hz) in which a CN anion is coordinated to the pincer complex (Fig. 2b). On the other hand, NO_3 complex **6d** shows a $^1J_{Pt-C}$ coupling constant ($^1J_{Pt-C}$ = 951 Hz) which is similar to the corresponding signal recorded for chloro complex **6a**. As a further test, when the chloro ligand in complex **6a** was replaced by the anionic OAc counterpart, the resulting platinum complex **6e** (X = OAc) shows a singlet at δ 139.0 ($^{13}C\{^1H\}$ NMR) with a $^1J_{Pt-C}$ coupling constant of 883 Hz.

These NMR studies clearly indicate that the organometallic C–Pt bonds in the pincer complexes are significantly influenced by the nature of *trans* donor atoms employed. A potential π-electron donor ligand, such as NO_3, tends to somewhat stabilize the organometallic Pt–C bond as determined by its respective Pt–P coupling constants. On the other hand, the Pt–C bonds are noticeably weakened by the *trans*-positioned CN and PR_3 ligands which are typically considered as electronic π-acceptors. Technically, it should be noted that no $^{13}C_{ipso}$–$^{13}C_{CN}$ couplings could be detected from CN complexes **6c**, **7c** and **8c**, due to the extremely low abundance of the required $^{13}C_{ipso}$–$^{13}C_{CN}$ fragments. Furthermore, the $^{13}C_{CN}$ signals are usually not discernible from the other aromatic carbon signals. It is interesting to note that in the corresponding $^{31}P\{^1H\}$ NMR study of PPh_3 complexes **6b**, **7b** and **8b**, all three complexes exhibited visibly weaker Pt–P coupling constants (2055–2085 Hz) for the Pt–P_{PPh_3} fragments than their Pt–P_{PPh_2} counterparts (2743–2775 Hz). Clearly, the aromatic rings induce stronger *trans* influence than the phosphorus atoms.

Consistent with the solution phase NMR observations, the solid state crystallographic study showed that the C_{ipso}–Pt bond in CN complex **6c** [2.062(5) Å] is longer than the corresponding organometallic bond of the two crystallographically independent molecules found in the single crystals of chloro complex **6a** [2.001(12) Å and 2.022(13) Å]. The observations from the solution NMR and solid state crystallographic studies indicated that some π back bonding may indeed be operating within the pincer C_{ipso}–Pt bonds (Fig. 3 and 4).

A classic approach towards tuning the electronic properties of a particular carbon atom within an aromatic ring is to introduce different substituents at the *para*-carbon positions. As shown in Table 1, the three cationic PPh_3 complexes **6b**, **7b** and **8b** exhibit very similar $^1J_{Pt-C}$ coupling constants (688, 688 and 703 Hz, respectively). Likewise, $^1J_{Pt-C}$ coupling constants are recorded within a small range (936–955 Hz) for the three neutral chloro complexes **6a**, **7a** and **8a**. The lack of noticeable electronic influence from the *para*-substituents is rather surprising. In order to confirm this observation, a very strong elec-

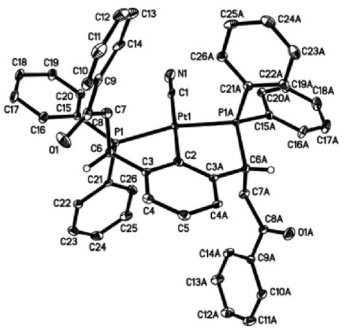

Fig. 3 Molecular structure of complex **6c**. All hydrogen atoms except H(C6) and H(C6A) are omitted for clarity.

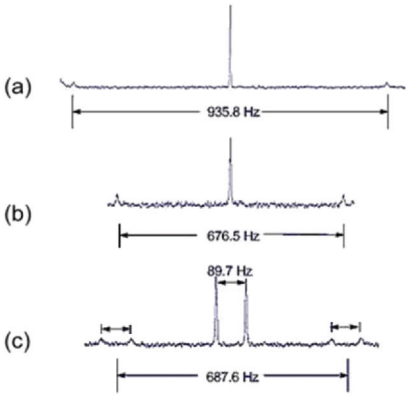

Fig. 2 $^{13}C\{^1H\}$ NMR signals for the Pt–C bonds in (a) complex **6a**, (b) complex **6c**, and (c) complex **6b**.

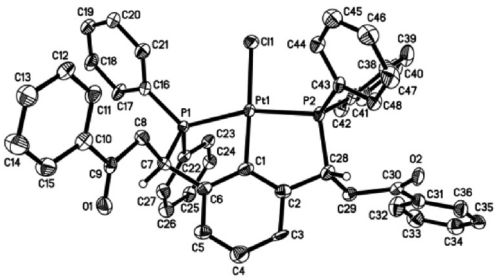

Fig. 4 Molecular structure of one independent molecule of complex **6a**. All hydrogen atoms except H(C7) and H(C28) are omitted for clarity. Another independent molecule which differs only slightly in bond angles and bond lengths, is shown in Fig. 45 of the ESI.†

tron-withdrawing fluorine atom was placed at the *para*-position to form complex **9a**. The resulting complex **9a** displays a singlet at δ 140.7 ($^{13}C\{^1H\}$ NMR) with a $^1J_{Pt-C}$ coupling constant of 951 Hz. A further confirmation was done by the introduction of the π-electron donating OMe group to form complex **10a**. This *para*-substituted OMe complex exhibits a singlet at δ 136.6 ($^{13}C\{^1H\}$ NMR) with a $^1J_{Pt-C}$ coupling constant of 952 Hz. Clearly, the electronic properties of the *para*-substituents in complexes **6–8** do not have significant effects on the organometallic C–Pt bonds.

To further investigate the subtle Pt–C interactions that cannot be evaluated directly by NMR spectroscopy, we conducted natural bond orbital (NBO)[9] analyses on complexes **6a** and **6c** at the B3LYP/[SDD(Pt),6-31G*(others)] level,[10,11] using the Gaussian 09 software package.[12] The NBO analysis identified two pairs of orbitals corresponding to the d(Pt)-to-π*(C) interactions for both **6a** and **6c** (Table 2). The sums of the π delocalization energies are 8.02 and 6.65 kcal mol^{-1} for **6a** and **6c**, respectively, as evaluated in a second-order perturbation fashion (for the identities of the NBO used for the second-order calculations, see Fig. 47 and 48 in the ESI†). The larger delocalization energy in **6a** is consistent with its shorter Pt–C bond distance.

As seen from the synthesized examples, the current series of PCP pincer platinum complexes show a high degree of flexibility for different types of monodentate ligands, such as NO_3 and PPh_3, to coordinate with the *trans* position of the C–M organometallic bonds. The above NMR and computational investigations clearly reveal the involvement of Pt → C π* back donation in these pincer complexes. This is probably the main driving force for the coordination of the classical "hard" oxy ligands to the typical soft platinum(II) centers.

It should be noted that the analogues of both type 1 and 2 complexes have been applied successfully in asymmetric hydrophosphination (AHP) reactions (Scheme 2).[5,7,13–15] Interestingly, both chiral catalysts required the presence of an additional base to activate the P–H bond in the asymmetric addition reaction. An external base such as triethylamine can be introduced to initiate the reaction, as illustrated in Scheme 1. Alternatively, an acetate anion associated with the catalysts can also serve as an effective internal base for the AHP process. From a mechanistic viewpoint, it is evident that the type 1 and 2 complexes operate *via* different catalytic pathways during the course of the AHP. A PC-cyclometalated complex (type 2) allows both the phosphine nucleophile and the reacting substrate to coordinate simultaneously with the metal center in the transition state. As a result, an intramolecular P–C bond formation mechanism is adopted.[7b] However, a pincer (type 1) catalyst offers only one easily accessible catalytic site; hence it is necessary for pincer complexes to adopt an intermolecular mechanism for an AHP reaction.[14a,15] In view of the current finding that oxy and phosphorus donors are able to coordinate to these pincer complexes, the pincer-catalyzed AHP could be triggered by either the P → Pt or the carbonyl–O → Pt interaction. In order to determine which mode of activation is involved when the platinum pincer complexes are used as catalysts in the P–H addition reaction with chalcone **11**, a series of closely monitored ^1H and $^{31}P\{^1H\}$ NMR experiments were conducted (see Fig. 42–44 in the ESI†).

Based on the ^1H NMR spectrum, the addition of chalcone **11** to pincer complex (*R*,*R*)-**6e** does not result in any visible chemical shifts in the proton signals of both the catalyst and substrate (see Fig. 42 in the ESI†). Furthermore, the proton signal arising from the –OAc group on **6e** remains unchanged at 1.92 ppm. Similarly, the $^{31}P\{^1H\}$ NMR studies indicate that no changes in the $^{31}P\{^1H\}$ chemical shift of complex **6e** was observed (when a stoichiometric amount of chalcone **11** was added to the NMR sample). However, in a separate sample, when a stoichiometric amount of Ph_2PH was introduced into complex **6e**, significant changes to the $^{31}P\{^1H\}$ chemical shifts are observed (see Fig. 43 and 44 in the ESI†). Subsequently, the reaction proceeded to completion upon addition of chalcone **11** to the NMR sample containing complex **6e** and $HPPh_2$. It should be noted that the same experimental observations were made in a previous study involving the analogous Pd(II) pincer complex.[15] In that report, it was also demonstrated that when PCP pincer ligand **1** was coordinated to the palladium(II) metal, these resulting Pd(II) pincer complexes could be used as reactive catalysts for hydrophosphination of activated olefins. It was observed that complex **6e** exhibits lower catalytic activity as compared to the analogous Pd(II) complex (X = OAc), indicating that the Pt–P (from Ph_2PH) bond formed during the course of the catalytic cycle is kinetically more stable than the corresponding Pd–P counterpart. The palladium catalysts also generated much higher ee (up to 43%) than complex **6e** (3% ee) when applied to the AHP of chalcone **11**.[13]

The conducted mechanistic investigations thus show that the platinum(II) pincer catalyst prefers to bind to phosphorus instead of the keto-moiety during the course of P–H addition

Table 2 NBO-based π-delocalization energy and DFT-derived *r*(Pt–C) for **6a** and **6c**

Species	π Delocalization energy (kcal mol^{-1})	*r*(Pt–C) (Å)
6a	8.02	2.045
6c	6.65	2.086

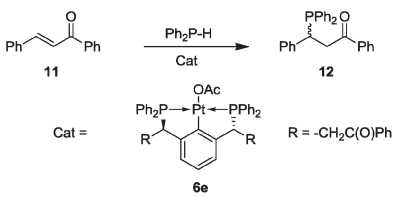

Scheme 2 Catalytic P–H addition reaction. (Note: A cat. loading of 5 mol% with chalcone **11** and $HPPh_2$ in DCM afforded the product **12** in 95% yield.)[13]

reaction. This experimental observation reveal that while the M → C π* character is inherently present in the pincer M–C bond, the back bonding nature is insufficient to render a high oxophilicity for the pincer catalyst to activate chalcone **11** *via* keto-O → M interactions. This is in contrast to the observation that the chalcone is activated *via* O → metal coordination when the *ortho*-metalated naphthalene (type 2) complexes were used as the catalysts for the same addition reaction.[7j] In fact the naphthalene (type 2) complexes prefer to form *trans* C(aryl)–M ← O bonds rather than the analogous C(aryl)–M ← P bonds.

Conclusions

In this work, a series of rationally designed Pt(II) pincer complexes were systematically examined to determine the electronic properties of the C(aryl)–M bonds. A study of the ^{13}C–^{195}Pt coupling constants of these complexes reveals the presence of significant π back-bonding operating within the pincer C–Pt bonds. The X-ray analysis and computational studies of selected complexes further substantiate the $^{13}C\{^1H\}$ NMR observations. NMR investigation conducted into the mode of activation (either P → Pt or carbonyl–O → Pt) in the pincer-catalyzed AHP reaction clearly indicates that the intermolecular addition of $HPPh_2$ to chalcone **11** proceeds *via* P → Pt interaction. Based on the current experimental and computational findings, we are currently developing a series of P–C–P transition metal pincer complexes with various functional groups on the side arms to allow for the fine-tuning of reactivity and stereoselectivity. These valuable complexes will be employed as catalysts for different types of asymmetric organic transformation reactions.

Experimental

All reactions were carried out under a positive pressure of nitrogen using the standard Schlenk technique. Solvents were purchased from the respective companies (DCM, THF: Fisher; toluene, *n*-hexanes: Avantor; acetone: Sigma-Aldrich) and used as supplied. Where necessary, solvents were degassed prior to use. A Low Temp Pairstirrer PSL-1800 was used for controlling low temperature reactions. Column chromatography was performed on Silica gel 60 (Merck). Melting points were measured using the SRS Optimelt Automated Point System SRS MPA100. Optical rotation was measured with an Atago automatic polarimeter (AP-300) in the specified solvent in a 0.1 dm cell at 589 nm. NMR spectra were recorded on Bruker AV 300 and AV 400 spectrometers at 300 K. Chemical shifts were reported in ppm and referenced to an internal $SiMe_4$ standard (0 ppm) or chloroform-d (7.26 ppm) for ^1H NMR, chloroform-d (77.23 ppm) for $^{13}C\{^1H\}$ NMR, and an external 85% H_3PO_4 for $^{31}P\{^1H\}$ NMR. All other reactants and reagents were used as supplied. The X-ray crystallographic examination and data collection were performed with Mo Kα radiation on a Bruker Kappa CCD spectrometer. Structure solution and refinement were done on a computer using the SHELX package.[16] PC-cyclometalated catalyst **A**,[7b] and complexes **9a** and **10a**[10] were prepared according to the literature methods. Pincer complexes **6a–8a** were prepared by the combination of a hydrophosphination protocol[7b] and a metalation procedure.[17]

General procedure for the synthesis of complexes 6a, 7a and 8a

To a solution of $HPPh_2$ (0.218 mmol, 1.0 eq.) in THF (3 mL) was added catalyst **A** (0.0109 mmol, 5 mol%) (see Scheme 1). The reaction mixture was stirred for complete dissolution and cooled to −80 °C. Dienone (0.107 mmol, 0.49 equiv.) was added, followed by a solution of NEt_3 (0.218 mmol, 1.0 equiv.) in THF (1 mL) dropwise. The reaction mixture was stirred overnight and monitored by $^{31}P\{^1H\}$ NMR for its completion. Upon completion, the reaction mixture was allowed to stand at room temperature and the solvent was removed under reduced pressure protected by nitrogen. The residue was dissolved in chloroform (10 mL) and $PtCl_2(PPh_3)_2$ (0.107 mmol, 0.49 eq.) was added. The reaction was stirred under reflux overnight. The reaction mixture was condensed to 2 mL and diluted with acetone (8 mL). KCl (0.214 mmol, 0.99 equiv.) and sulfur (0.214 mmol, 0.99 equiv.) were added. The mixture was refluxed for 2 h and evaporated under reduced pressure to give the crude product, which was then purified by silica gel column chromatography to afford the pure complex.

General procedure for the synthesis of complexes 6b, 7b and 8b

To a solution of pincer-Pt–Cl complex **6a**, **7a** or **8a** (0.0505 mmol, 1.0 equiv.) in DCM (5 mL) and water (1 mL) were added PPh_3 (0.0505 mmol, 1.0 equiv.) and $AgClO_4$ (0.101 mmol, 2.0 equiv.) The reaction mixture was stirred for 2 h. The residue was removed and the filtrate was washed with water (2 × 20 mL), dried over Na_2SO_4 and concentrated to give the crude product, which was purified by silica gel column chromatography.

General procedure for the synthesis of complexes 6c, 7c and 8c

To a mixture of pincer-Pt–Cl complex **6a**, **7a** or **8a** (0.042 mmol, 1.0 equiv.) in DCM (5 mL) and water (1 mL) was added AgCN (0.084 mmol, 2.0 equiv.). The reaction mixture was stirred overnight, filtered through celite and the filtrate was washed with water, dried over Na_2SO_4 and concentrated to give the crude product, which was purified by silica gel column chromatography.

General procedure for the synthesis of complexes 6d, 7d and 8d

To a solution of pincer-Pt–Cl complex **6a**, **7a** or **8a** (0.213 mmol, 1.0 equiv.) in chloroform (10 mL) and water (2 mL) was added $AgNO_3$ (0.850 mmol, 4.0 equiv.). The reaction mixture was stirred overnight. The residue was removed by filtration and the filtrate was washed with water, dried over Na_2SO_4 and concentrated to give the pure product.

Synthesis of complex 6e

To a solution of pincer-Pt–Cl complex **6a** (0.213 mmol, 1.0 equiv.) in DCM (10 mL) was added AgOAc (0.320 mmol, 1.5 equiv.). The reaction mixture was stirred overnight, filtered through a plug of silica gel and extracted into DCM (25 mL). The organic layer was washed with water (2 × 25 mL), dried over Na_2SO_4 and concentrated to give the pure product **6e**.

General procedure for catalytic addition of diphenylphosphine to chalcone

Catalyst **6e** (25 μmol, 5 mol%) was added to a solution of diphenylphosphine (0.5 mmol, 1.0 equiv.) in DCM (1 mL) and stirred at RT followed by subsequent addition of chalcone **11** (0.5 mmol, 1.0 equiv.). Completion of the reaction was determined by the disappearance of the phosphorous signal attributed to diphenylphosphine (−40 ppm) in the $^{31}P\{^1H\}$ NMR spectrum. Upon completion of the reaction, aq. H_2O_2 (0.1 mL, 31% v/v) was added to form the respective product. The volatiles were removed under reduced pressure and the crude product was directly loaded onto a silica gel column (3EA : 2*n*-hexane) to afford the pure product. The data obtained is consistent with the literature.[7c]

Computational methods

DFT calculations and NBO analyses were performed on complexes **6a** and **6c**, which show distinct C–Pt bond lengths (see above). The B3LYP functional was used in conjunction with the SDD effective core potential basis set (for Pt) and the 6-31G* basis set (for the other atoms).[10,11] This level of theory is referred to here as B3LYP/[SDD(Pt),6-31G*(others)]. Calculations were performed using the Gaussian 09 software package.[12] NBO analyses were performed on DFT optimized geometries using the NBO program version 3.1 implemented in Gaussian 09.

Acknowledgements

We are grateful to Nanyang Technological University for supporting this research and the research scholarships to Y.-X. J and X.-Y. Y.

Notes and references

1 For selected reviews, see: (*a*) G. Erre, S. Enthaler, K. Junge, S. Gladiali and M. Beller, *Coord. Chem. Rev.*, 2008, **252**, 471; (*b*) M. S. Shaharun, B. K. Dutta, H. Mukhtar and S. Maitra, *Chem. Eng. Sci.*, 2010, **65**, 273; (*c*) D. K. Dutta and B. Deb, *Coord. Chem. Rev.*, 2011, **255**, 1686; (*d*) B. Bosnich, *Acc. Chem. Res.*, 1998, **31**, 667; (*e*) *Phosphorous Ligands in Asymmetric Catalysis*, ed. A. Börner, Wiley-VCH, Weinheim, 2008, vol. I–III.

2 For recent reviews, see: (*a*) K. J. Szabó, *Top. Organomet. Chem.*, 2013, **40**, 203; (*b*) D. M. Roddick, *Top. Organomet. Chem.*, 2013, **40**, 49; (*c*) *Organometallic Pincer Chemistry, Topics in Organometallic Chemistry*, ed. G. van Koten and D. Milstein, Springer-Verlag, Berlin, Heidelberg, 2013; (*d*) N. Selander and K. J. Szabó, *Chem. Rev.*, 2011, 111, 2048; (*e*) *Phosphorous(III) Ligands in Homogeneous Catalysis: Design and Synthesis*, ed. P. C. J. Kamer and P. W. N. M. van Leeuwen, Wiley-VCH, Weinheim, Germany, 2012; (*f*) B. Rybtchinski and D. Milstein, *Angew. Chem., Int. Ed.*, 1999, **38**, 870; (*g*) M. E. van der Boom and D. Milstein, *Chem. Rev.*, 2003, **103**, 1759.

3 For a recent review, see: (*a*) D. M. Roddick, *Top. Organomet. Chem.*, 2013, **40**, 49; For examples of (PCP)Pd systems, see: (*b*) J. L. Bolliger, O. Blacque and C. M. Frech, *Angew. Chem., Int. Ed.*, 2007, **46**, 6514; (*c*) R. Gerber, T. Fox and C. M. Frech, *Chem. – Eur. J.*, 2010, **16**, 6771; (*d*) J. L. Bolliger, O. Blacque and C. M. Frech, *Chem. – Eur. J.*, 2008, **14**, 7969; For examples of (PCP)Pt systems, see: (*e*) J. J. Adams, A. Lau, N. Arulsamy and D. M. Roddick, *Inorg. Chem.*, 2007, **46**, 11328; (*f*) D. Vuzman, E. Poverenov, Y. Diskin-Posner, G. Leitus, L. J. W. Shimon and D. Milstein, *Dalton Trans.*, 2007, 5692; For examples of (PCP)Ir systems, see: (*g*) J. J. Adams, N. Arulsamy and D. M. Roddick, *Organometallics*, 2011, **30**, 697; (*h*) I. Goettker-Schnetmann, P. S. White and M. Brookhart, *Organometallics*, 2004, **23**, 1766; (*i*) S. M. Kloek, D. M. Heinekey and K. I. Goldberg, *Organometallics*, 2006, **25**, 3007.

4 B. J. Coe and S. J. Glenwright, *Coord. Chem. Rev.*, 2011, **255**, 1686.

5 Y.-X. Jia, B.-B. Li, Y. Li, S. A. Pullarkat, K. Xu, H. Hirao and P. H. Leung, *Organometallics*, 2014, **33**, 6053.

6 (*a*) P. H. Leung, *Acc. Chem. Res.*, 2004, **37**, 169; (*b*) P. H. Leung, S. K. Loh, K. F. Mok, A. J. P. White and D. J. Williams, *J. Chem. Soc., Chem. Commun.*, 1996, **42**, 591; (*c*) P. H. Leung, G. He, H. Lang, A. Liu, S. K. Loh, S. Selvaratnam, K. F. Mok, A. J. P. White and D. J. Williams, *Tetrahedron*, 2000, **56**, 7.

7 (*a*) S. A. Pullarkat and P.-H. Leung, *Top. Organomet. Chem.*, 2013, **43**, 145; (*b*) Y. Huang, R. J. Chew, Y. Li, S. A. Pullarkat and P. H. Leung, *Org. Lett.*, 2011, **13**, 5862; (*c*) Y. Huang, S. A. Pullarkat, Y. Li and P.-H. Leung, *Inorg. Chem.*, 2012, **51**, 2533; (*d*) Y. Huang, R. J. Chew, S. A. Pullarkat, Y. Li and P.-H. Leung, *J. Org. Chem.*, 2012, **77**, 6849; (*e*) R. J. Chew, Y. Huang, Y. Li, S. A. Pullarkat and P.-H. Leung, *Adv. Synth. Catal.*, 2013, **355**, 1403; (*f*) Y. Huang, Y. Li, P.-H. Leung and T. Hayashi, *J. Am. Chem. Soc.*, 2014, **136**, 4865; (*g*) R. J. Chew, Y. Lu, Y.-X. Jia, B.-B. Li, E. H. Y. Wong, R. Goh, Y. Li, Y. Huang, S. A. Pullarkat and P.-H. Leung, *Chem. – Eur. J.*, 2014, **20**, 14514; (*h*) R. J. Chew, K. Y. Teo, Y. Huang, B.-B. Li, Y. Li, S. A. Pullarkat and P.-H. Leung, *Chem. Commun.*, 2014, **50**, 8768; (*i*) R. J. Chew, X.-R. Li, Y. Li, S. A. Pullarkat and P.-H. Leung, *Chem. – Eur. J.*, 2015, **21**, 4800; (*j*) Y. Huang, S. A. Pullarkat, Y. Li and P.-H. Leung, *Chem. Commun.*, 2010, **46**, 6950.

8 P. E. Garrou, *Chem. Rev.*, 1981, **81**, 229.

9 (*a*) A. E. Reed, L. A. Curtiss and F. Weinhold, *Chem. Rev.*, 1988, **88**, 899; (*b*) E. D. Glending, C. R. Landis and F. Weinhold, *WIREs Comput. Mol. Sci.*, 2012, **2**, 1.

10 (*a*) A. D. Becke, *J. Chem. Phys.*, 1993, **98**, 5648; (*b*) C. Lee, W. Yang and R. G. Parr, *Phys. Rev. B: Condens. Matter Mater. Phys.*, 1988, **37**, 785; (*c*) S. H. Vosko, L. Wilk and M. Nusair, *Can. J. Phys.*, 1980, **58**, 1200; (*d*) A. D. Becke, *Phys. Rev. B: Condens. Matter Mater. Phys.*, 1988, **38**, 3098; (*e*) P. J. Stephens, F. J. Devlin, C. F. Chablowski and M. Frisch, *J. Phys. Chem.*, 1994, **98**, 11623.

11 (*a*) W. Hehre, L. Radom, P. V. R. Schleyer and J. A. Pople, *Ab Initio Molecular Orbital Theory*, John Wiley & Sons, New York, 1986; (*b*) M. Dolg, U. Wedig, H. Stoll and H. Preuss, *J. Chem. Phys.*, 1987, **86**, 866.

12 M. J. Frisch, G. W. Trucks, H. B. Schlegel, G. E. Scuseria, M. A. Robb, J. R. Cheeseman, G. Scalmani, V. Barone, B. Mennucci, G. A. Petersson, H. Nakatsuji, M. Caricato, X. Li, H. P. Hratchian, A. F. Izmaylov, J. Bloino, G. Zheng, J. L. Sonnenberg, M. Hada, M. Ehara, K. Toyota, R. Fukuda, J. Hasegawa, M. Ishida, T. Nakajima, Y. Honda, O. Kitao, H. Nakai, T. Vreven, J. A. Montgomery Jr., J. E. Peralta, F. Ogliaro, M. Bearpark, J. J. Heyd, E. Brothers, K. N. Kudin, V. N. Staroverov, T. Keith, R. Kobayashi, J. Normand, K. Raghavachari, A. Rendell, J. C. Burant, S. S. Iyengar, J. Tomasi, M. Cossi, N. Rega, J. M. Millam, M. Klene, J. E. Knox, J. B. Cross, V. Bakken, C. Adamo, J. Jaramillo, R. Gomperts, R. E. Stratmann, O. Yazyev, A. J. Austin, R. Cammi, C. Pomelli, J. W. Ochterski, R. L. Martin, K. Morokuma, V. G. Zakrzewski, G. A. Voth, P. Salvador, J. J. Dannenberg, S. Dapprich, A. D. Daniels, O. Farkas, J. B. Foresman, J. V. Ortiz, J. Cioslowski and D. J. Fox, *GAUSSIAN 09 (Revision B.01)*, Gaussian, Inc., Wallingford, CT, 2010.

13 X.-Y. Yang, W. S. Tay, S. A. Pullarkat and P.-H. Leung, *Organometallics*, 2015, **34**, 1582.

14 For selected examples, see: (*a*) J.-J. Feng, X.-F. Chen, M. Shi and W.-L. Duan, *J. Am. Chem. Soc.*, 2010, **132**, 5562; (*b*) J. Lu, J. Ye and W.-L. Duan, *Org. Lett.*, 2013, **15**, 5016; (*c*) B. Ding, Z. Zhang, Y. Xu, Y. Liu, M. Sugiya, T. Imamoto and W. Zhang, *Org. Lett.*, 2013, **15**, 5476.

15 X.-Y. Yang, J. H. Gan, Y. Li, S. A. Pullarkat and P.-H. Leung, *Dalton Trans.*, 2015, **44**, 1258.

16 G. M. Sheldrick, *Acta Crystallogr., Sect. A: Found. Crystallogr.*, 2008, **64**, 112.

17 F. Gorla and L. M. Venanzi, *Organometallics*, 1994, **13**, 43.